



An Advanced Lead Rubber Bearing Analytical Model Under Low and High Shear Strain Level

Vahid Aghaeidoost¹ and AHM Muntasir Billah^{2*}

¹PhD Student, Department of Civil Engineering, University of Calgary, Calgary, Canada

²Assistant Professor, Department of Civil Engineering, University of Calgary, Calgary, Canada

*muntasir.billah@ucalgary.ca (Corresponding Author)

ABSTRACT

Seismic isolation devices have been widely used for improving the seismic performance of bridges while reducing the expected damage. One of the most widely used seismic isolation systems is the lead rubber bearing (LRB). As a result, several analytical models of LRB exist in the literature. However, each of them has their own advantages and disadvantages. While some models perform better under low shear strain but unable to capture the bearing response under large shear strain and vice versa. Again, some models can predict the strength and stiffness degradation under seismic loading while other can't. In order to ensure adequate performance of the base-isolated structure, the behavior of isolation systems should be predictable for all possible loading conditions and the isolation system should maintain its functionality at greater than the design level hazard with a high confidence. This research focuses on developing a nonlinear model of LRB to capture the complicated nonlinear behavior of LRBs at low and high shear strains under seismic loading to accurately predict isolator displacements and overall response of base-isolated bridges. The main focus is to develop a new analytical model for LRB which is able to capture all aspects of LRB response in one model, such as the initial lead core hardening, strength degradation due to the lead core heating, rubber hardening, large strain effect, and Scragging and Mullins effects, which are absent in existing models. The developed analytical model has been validated against experimental results. The comparative analyses demonstrated the high efficacy of the developed model in predicting LRB responses under high and low shear strains.

Keywords: Lead rubber bearing, large shear strain, analytical model, rubber hardening, lead core heating, and Scragging and Mullins effects.

INTRODUCTION

Seismic protection systems aim to reduce the impact of earthquakes on structures and infrastructures. This is done by implementing techniques such as base isolation and energy dissipation devices to enhance the seismic resistance of the structures. Base isolation bearings are commonly used for seismic protection purposes, with the Lead Rubber Bearing (LRB) being the most popular method [1] in base-isolated structures due to its substantial energy dissipation capability [2–4] and straightforward assembly. LRBs consist of alternating layers of rubber and steel shims with a central lead core constrained between the top and bottom steel plates, which enables energy dissipation through core yielding [5]. The combination of features in LRBs renders them an efficient and widely implemented seismic isolation system.

Researchers have developed various analytical and numerical models to study the complicated nonlinear behavior of LRBs under dynamic loading. To develop models that can accurately depict LRB behavior under low-to-high amplitude cyclic displacements, a comprehensive review of existing studies on the characteristics of LRBs were conducted. It is found that the reduction in strength due to lead core heating, initial lead core hardening, rubber hardening, unloading effect, strain rate-dependency of skeleton curve, and Scragging and Mullins damage effects are important characteristics to consider. It is also found that it is crucial to have a model that captures both the hardening effects and the softening unloading effects. Despite some models being able to capture essential features, a model that can fully capture the complex nonlinear behavior of LRBs under low-to-high strain rate is yet to be developed. This study aims to address the deficiencies in existing models by gaining a thorough understanding of them to identify the sources of nonlinear behavior exhibited in LRBs.

REVIEW OF EXISTING MODELS

This section provides a brief overview of different LRB analytical models developed to date. The Bouc-Wen model [6,7] is a widely-used analytical model in structural engineering for simulating hysteretic systems including the LRBs hysteresis curve employed to describe non-linear hysteretic systems. In this model, unlike the bi-linear model, stiffness transitions between pre- and post-yield are accurately captured, as well as the potential hardening effects that can occur in various systems [8]. Kikuchi and Aiken [9] proposed an analytical LRB model to predict the seismic response of base-isolated structures. However, this model is not able to account for the initial hardening of lead and rubber, as well as the Scragging and Mullins effect. Kalpakidis and Constantinou [10,11] developed a more advanced model for LRBs that is able to capture the heating effect on the strength of the lead core. This variation of the model is based on the Bouc-Wen formulation and allows for the degradation of hysteresis due to cyclic loading. A temperature-tensile strength relationship along with several assumptions was used to calculate the relationship between strength degradation and cyclic displacement.

Eem and Hahm [12] proposed an analytical model of LRB that was validated through full-scale testing under various strain levels, but it still had some limitations. Marquez et al. [13] proposed a new approach that incorporated factors such as strength degradation, rubber strain hardening, and unloading effects to predict the behavior of LRBs under large strains. Chen et al. [14] proposed a generalized Bouc-Wen model that can capture the large strain stiffening and strength degradation properties of rubber in LRBs. The model was compared with the experimental results of LRBs with various design parameters under different loading conditions. However, each of these proposed models has its own limitations and constraints, such as neglecting the initial hardening of lead, not accounting for rubber hardening, and not fully incorporating rate-dependency and strength degradation due to the lead core heating.

The main aim of this study is to develop a nonlinear model that can effectively predict the comprehensive response and displacements of lead rubber bearings (LRBs) in a precise manner. The proposed model accounts for various factors that have an impact on the response of LRBs, including lead hardening during the initial phase, strength degradation that is caused by lead core heating, rubber hardening, the effects of large strain, rate-dependency of skeleton curve, the softening unloading effect, the vertical load effect, and the Scragging and Mullins damage parameters effect. The reliability and accuracy of the proposed model have been evaluated by comparing with large-scale experimental results. The study findings could be useful in practical applications, particularly in the design and implementation of base-isolated highway bridges, which can then be better equipped to withstand natural hazards.

METHODOLOGY

This section describes the methodology used to develop the LRB analytical model in a step-by-step manner while explaining the parameters and features that influence the behavior of LRBs. Figure 1 illustrates the essential features of LRB behavior extracted from previous experimental study.

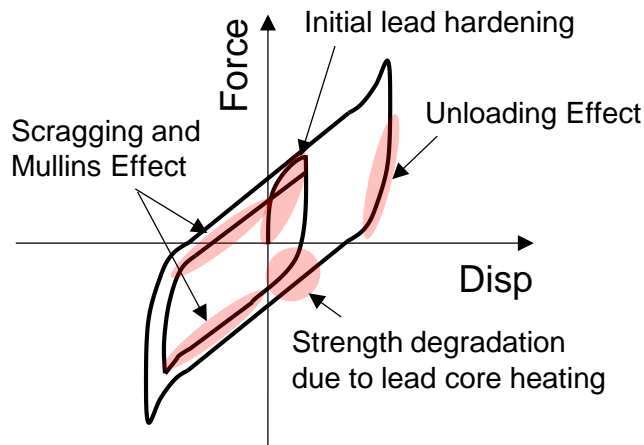


Figure 1. LRB behavioral features extracted from previous experimental tests.

Lead core heating

The lead rubber bearings can degrade in strength due to the lead core heating, which can cause the lead core to expand and reduce the bearing's stiffness. The compression and distortion of rubber resulting from lead core heating can also negatively affect the bearing's performance by reducing its elasticity and increasing stiffness. Kalpakidis and Constantinou [15]

investigated the relationship between the temperature of a lead core and its shear strength and developed a mathematical formulation for calculating the heating resulting from cyclic loading. This formulation was integrated into Opensees and was later improved by Kumar et al. [16]. This bi-directional, coupled Bouc-Wen model allows for a degradation in hysteresis based on the Bouc-Wen formulation, which captures the effect of lead core heating on the temperature-lead strength relationship. Eq. (1) represents the forces (ΔF) associated with lead core heating that are added to restoring forces:

$$\Delta F = (\sigma_{YL}(T_L)A_L) \cdot Z \quad (1)$$

The dimensionless parameters Z in Eq. (1) are limited by ± 1 . According to Park et al. [17], this formulation extends the Bouc-Wen model by capturing the biaxial interaction between hysteretic systems. As described in Kalpakidis and Constantinou [15], cyclic displacement and strength degradation are thermodynamically related using an experimental temperature-strength relationship. The lead core strength degradation is expressed as $\sigma_{YL}(T_L)$ in Eq. (2):

$$\sigma_{YL}(T_L) = \sigma_{YL0} \cdot e^{-E_2 T_L} \quad (2)$$

where T_L is the temperature of the lead, σ_{YL0} is the effective yield stress of lead at the reference (starting) temperature, and E_2 is the rate of degradation.

Damage parameters

The Scragging effect and the Mullins effect are two scientific phenomena that can negatively impact the performance of isolation bearings which are proposed by Grant et al. [18]. The Scragging effect occurs when the rubber material in the bearing is deformed under high loads and/or high temperatures, leading to a loss of elasticity and an increase in stiffness. This can reduce the load capacity of the bearing and lead to premature failure. The Mullins effect, on the other hand, occurs over time as a result of constant deflection, causing a gradual reduction in the elasticity of the rubber material and resulting in permanent deformation. This can also lead to a loss of load capacity and increased stiffness. The model incorporates both effects into its hysteretic formulations, which take into account the damage parameters effects. Exponential degradation equations (Eqs. 3-5) are used to formulate the equations, which describe the gradual reduction in the elasticity of the rubber material due to the Scragging and Mullins effects. These equations help to predict the behavior of the isolation bearing over time and can be used to optimize its design and performance.

$$K_{S1} = e^{-c_1 D_S^3} \quad (3)$$

$$K_{S2} = e^{-c_2 D_S^3} \quad (4)$$

$$K_M = c_3 + (1 - c_3)e^{-c_4 D_M^3} \quad (5)$$

These equations are described by parameters c_1 to c_4 and are calibrated by test results. K_{S1} and K_M are damage parameters factors in the model that impact the hysteresis component, while K_{S2} impacts the plasticity component, particularly the hardening in the bounding surface. Parameters c_1 and c_2 account for the degradation caused by Scragging effects, while parameters c_3 and c_4 account for the degradation caused by the Mullins damage effect. Other two parameters, c_4 represents the damage rate, and c_3 , can vary from zero to one that determines the damage limit. The Scragging damage parameter, D_S , indicates the permanent damage caused to the bearing, while D_M is the damage parameter for Mullins' effect.

Initial lead strain hardening

LRBs demonstrate a phenomenon called initial lead hardening. This occurrence has been overlooked in previous models, and thus, we aim to investigate it further. This is a phenomenon that occurs as a result of the lead core in the bearing being compressed during installation. This compression causes the lead to become denser and more rigid, which can lead to an increase in stiffness and a reduction in the overall load capacity of the bearing. This initial hardening effect is temporary and will decrease as the lead core relaxes and the bearing is loaded. It is proposed that a new phenomenological model that has been modified from the damage model introduced by Grant et al. [18] is presented to address this issue. The typical hysteretic force formulation is outlined in Eq. (6) [13].

$$K_I = 1 - c_5 e^{-c_6 D_I} \quad (6)$$

The inverse of a conventional damage parameter, such as Mullins' and Scragging parameter discussed in Grant et al [18], is utilized in this equation. D_I , a parameter that increases with displacement increments akin to the distance traveled, is employed. While c_6 can take on any positive value, c_5 is a user-defined parameter that ranges between zero and one. These parameters are

calibrated according to experimental test results from Eem and Hahm [12]. Thus, the model initially predicts a low yield point and gradually approaches the actual strength as D_I increases, ultimately resulting in K_I approaching one.

Rubber strain hardening

The hardening of rubber within isolation bearings occurs due to the application of heat and load over a period of time. These factors cause the molecular structure of the rubber to deteriorate, rendering the material more susceptible to becoming brittle. This alteration can result in a reduction in the material's elasticity and an increase in stiffness, both of which can have detrimental effects on the performance of the isolation bearing.

Hysteresis component model

This section discusses an analytical hysteresis component model for LRBs to predict the seismic response of base-isolated structures. The stiffness and damping functions of the bearings were described based on shear strain, and the parameters of the models were updated according to the maximum shear strain at the unloading point from the skeleton curve to ensure that the stiffness and damping values in the analytical model matched the empirical values. It is found that existing models such as the modified bilinear model, the modified Ramberg-Osgood model, and differential equation-based models such as the Ozdemir model [19] and the Wen model [7] were not able to accurately capture the non-linear stiffening behavior of elastomeric bearings when subjected to high levels of shear strain.

Therefore, Kikuchi and Aiken [9] proposed the following equations as an effective model for modeling the behavior of LRBs over a wide range of strains. These equations improve performance at high levels of shear strain. However, the proposed model does not consider the effects of strain rate, Scragging and Mullins damage effects, and initial lead hardening on the hysteresis properties of the bearings.

$$\mathbf{F} = \mathbf{F}_1 + \mathbf{F}_2 \quad (6)$$

$$\mathbf{F}_1 = \frac{1}{2}(1 - \mathbf{u})\mathbf{F}_m\{\mathbf{x} + \mathbf{sgn}(\dot{\mathbf{X}})|\mathbf{x}|^n\} \quad (7)$$

$$\mathbf{F}_2 = \begin{cases} \mathbf{u}\mathbf{F}_m\{1 - 2e^{-a(1+\mathbf{x})} + b(1 + \mathbf{x})e^{-c(1+\mathbf{x})}\}, \dot{\mathbf{X}} > 0 \\ -\mathbf{u}\mathbf{F}_m\{1 - 2e^{-a(1-\mathbf{x})} + b(1 - \mathbf{x})e^{-c(1-\mathbf{x})}\}, \dot{\mathbf{X}} < 0 \end{cases} \quad (8)$$

The skeleton curve exhibits a maximum shear force denoted by F_m , whereas the normalized shear displacement is represented by x ($x = X/X_m$), with X_m being the maximum shear displacement on the skeleton curve. The stiffening behavior which is rate-dependent is characterized by the parameter n in Eq. (7). Eq. (8) employs the parameter u , which is the ratio of the shear force at zero displacement, F_u , to the maximum shear force, F_m ($u = F_u/F_m$). The parameters a and b are obtained through specific calculations. These equations are based on the assumption of equivalent hysteresis loop areas for analytical and experimental data.

PROPOSED MODEL

The comprehensive model introduced in this section is able to model all the features required for capturing the complex nonlinear behavior of the LRBs. Thus, in Eq. (9), three components of skeleton curve behavior, hysteretic component and the effect of strength degradation due to lead core heating in cyclic loads are observed. In addition, in Eq. (10), where the skeleton curve component is introduced, the effect of Scragging and Mullins's damage parameters is presented, which will finally be modified by taking into account the rate-dependence of the hardening parameter of the final shape. Finally, in Eq. (11) hysteretic components, in which the initial hardening effect of the lead core and rubber, as well as the Scragging damage parameter, reversal load behavior and unloading are also included. This model is able to accurately predict the behavior of LRBs at low and high strain rates. The Figure 2 demonstrates the components of the proposed model including: skeleton curve and hysteresis components.

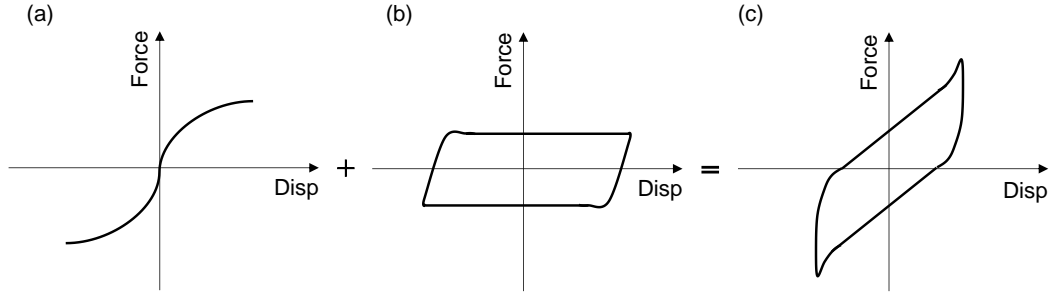


Figure 2. Proposed model: (a) Skeleton curve, (b) Hysteresis component, and (c) Nonlinear behavior of LRBs.

$$\mathbf{F} = \mathbf{F}_1 + \mathbf{F}_2 + \Delta\mathbf{F} \quad (9)$$

$$\mathbf{F}_1 = \frac{1}{2} K_{S1} K_M (1 - u) F_m \{x + \text{sgn}(X) |x|^n\} \quad (10)$$

$$\mathbf{F}_2 = \begin{cases} u K_I F_m \{1 - 2e^{-a(1+x)} + b K_{S2} (1+x) e^{-c(1+x)}\}, \dot{X} > 0 \\ -u K_I F_m \{1 - 2e^{-a(1-x)} + b K_{S2} (1-x) e^{-c(1-x)}\}, \dot{X} < 0 \end{cases} \quad (11)$$

COMPARISON AND DISCUSSION OF DEVELOPED MODEL

The behavior of LRBs are discussed in this section, which are used in the seismically isolated structures. Hysteresis curves are commonly used to study the behavior of LRBs under cyclic loading and provide valuable information about the effective damping ratio and effective stiffness of the LRBs. The effective damping ratio represents the energy dissipation capacity of the LRB, while the effective stiffness represents its ability to resist deformation. The behavior of LRBs under cyclic loading is compared using these parameters and comprehensive comparison of the hysteresis curves obtained from an experimental model and a proposed model for LRBs are provided in this section. Figure 3a, b and Figure 4a, b depict the comparison of the proposed analytical model and experimental results from Eem and Hahm [12] in terms of force-time history and force-displacement hysteresis at 100% (low strain) and 500% (high strain) strain rate, respectively.

Figure 3a depicts a comparative analysis of the force-time history response under 100% strain rate, where a notable correspondence is evident between the forces yielded by the proposed model and those observed in the experimental domain. Only in the ultimate stages of the test, the force value of the proposed model is underestimated and exhibits a 25% deviation. Figure 3b, on the other hand, portrays a similar comparison between the force-displacement hysteresis behavior, at the same strain rate. As apparent from the curve, the upper and lower bounds of displacement and force are accurately estimated, and the unloading effect, rubber hardening, initial lead hardening, as well as the effects of Scragging and Mullins damages are also precisely accounted for. The results obtained at this strain rate are in good agreement with the experimental results.

At high strain rate (500%), the comparative analysis of the experimental results and the proposed model reveals that the proposed model exhibits a significant level of accuracy in predicting the experimental forces. This trend persists throughout the loading period (Figure 4a). In addition, Figure 4b, by comparing the force-displacement hysteresis of the proposed model with the experimental results, shows that the proposed model is able to estimate the upper and lower bounds of the forces and displacements with remarkable accuracy, as well as the initial lead hardening, unloading effect, rubber hardening, and Scragging and Mullins damage effects are also precisely predicted. This figure demonstrates the high accuracy of the proposed model at high strain rates in predicting the behavior of LRBs.

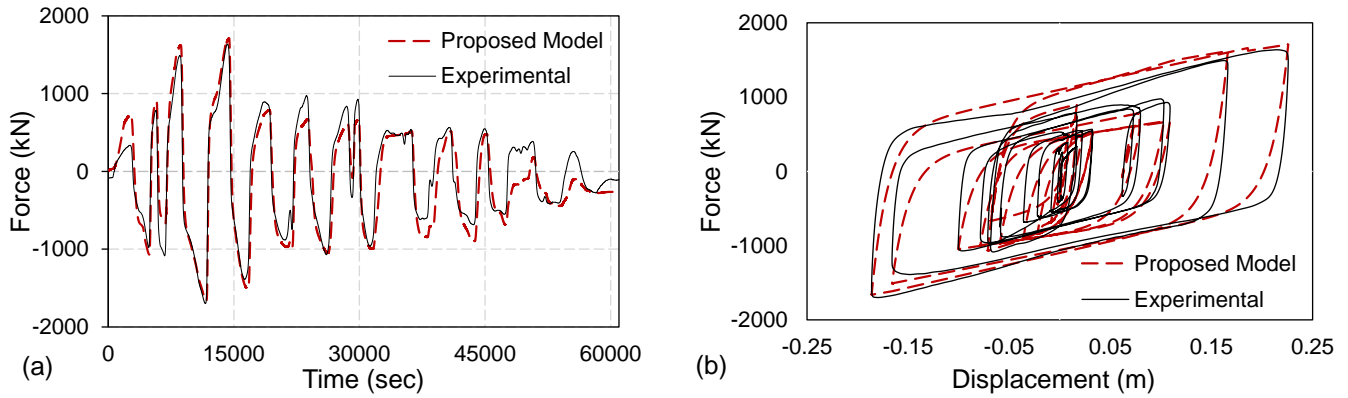


Figure 3. Comparison of Eem and Hahm experimental results [12] and proposed model (a) Force-time history and (b) Hysteresis curve under 100 % strain rate.

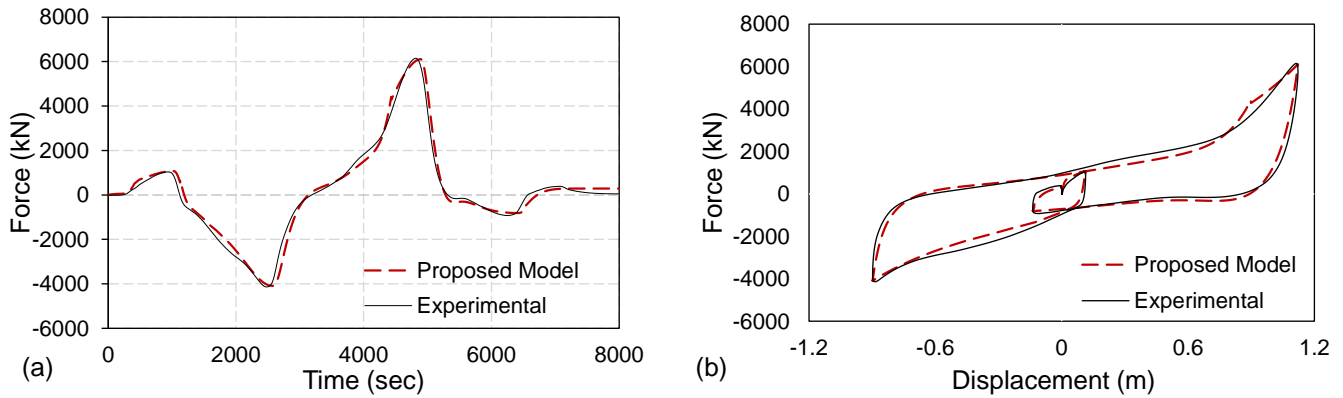


Figure 4. Comparison of Eem and Hahm experimental results [12] and proposed model (a) Force-time history and (b) Hysteresis curve under 500 % strain rate.

Table 1 represents the error comparison between the experimental results and proposed model under low and large strain rates. The results demonstrate that the accuracy of proposed model to capture the behavior of LRBs is significantly high. For example, at low strain rate the dissipated energy and hysteresis damping constant are only 7.94% and 1.02% deviant from the experimental results, respectively. Also, at large strain rates the dissipated energy and hysteresis damping constant are only 5.52% and 0.86% deviant from the experimental results, respectively.

Table 1. Error comparison of proposed model and Eem and Hahm [12] experimental results.

Strain Rate	Dissipated energy (%)	Hysteresis Damping Constant (%)
Low strain rate (100%)	7.94	1.02
High strain rate (500%)	5.52	0.86

Figures 5-6 compare the effective damping ratio (β_{eff}) and effective stiffness (K_{eff}) of LRBs obtained from the experiment under 100% and 500% strain and the values obtained from the proposed analytical model. Based on the results shown in Figure 5, both the experimental model and proposed model have similar damping characteristics under low amplitude loads (100%). However, under high amplitude loads, the experimental model has higher damping properties than the proposed model, while the proposed model has significantly accurate prediction on stiffness properties. The analysis revealed that the proposed model has greater accuracy in predicting the effective stiffness value for the first seven cycles and the effective damping ratio for the first four cycles. However, a decrease in the accuracy of the effective damping ratio and stiffness value predictions was observed from the 7th cycle onwards. Furthermore, as the number of cycles increased, the proposed model's predictive accuracy for both effective damping ratio and stiffness value decreased. Notably, the accuracy of the effective stiffness and damping ratio for primary cycles aligned significantly with the experimental data. For instance, the effective damping ratios difference between proposed model and experimental results at cycle 3, 6, and 9 are 1.27%, 2.81%, and 4.97%, while the effective stiffness differences are 2.22%, 2.23%, and 8.74%, respectively. In Figure 6, for high strain loads (500%), two sets of experimental and proposed models are compared for their effective damping ratio and effective stiffness. For the first cycle, the proposed model showed slightly less effective damping ratio and similar effective stiffness. This trend continued for the second cycle as well. Therefore, the experimental model demonstrated higher damping properties than the proposed model. For example, the

difference between proposed model and experimental results for cycle 1 and 2 are 0.88% and 0.34% for effective damping ratio and 1.15% and 0.67% for effective stiffness, respectively.

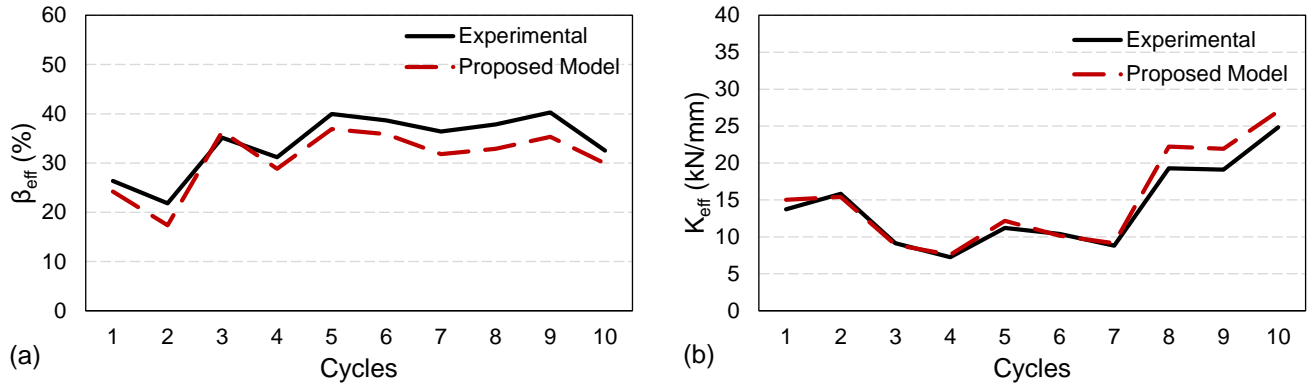


Figure 5. Comparison of Eem and Hahm experimental results [12] and proposed model (a) Effective Damping Ratio and (b) Effective Stiffness for different cycles under 100 % strain rate.

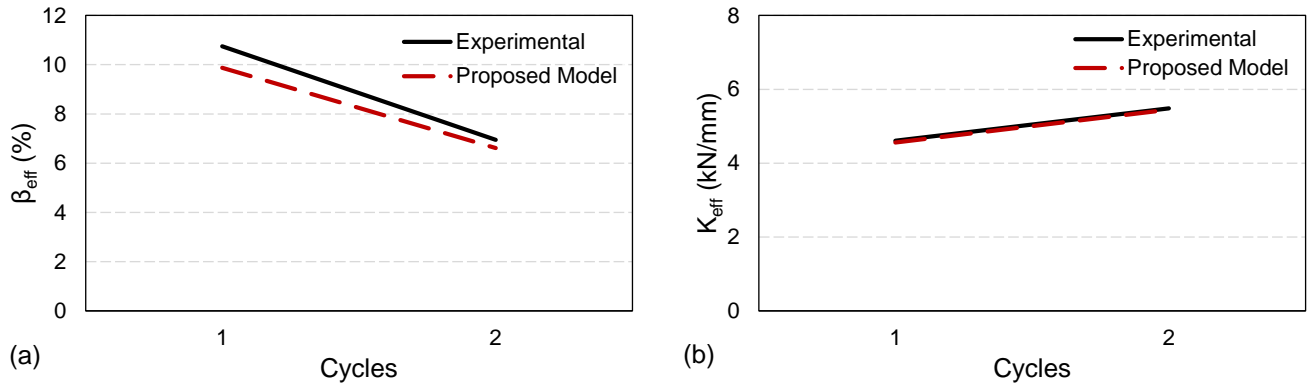


Figure 6. Comparison of Eem and Hahm experimental results [12] and proposed model (a) Effective Damping Ratio and (b) Effective Stiffness for different cycles under 500 % strain rate.

CONCLUSIONS

In this research, a new nonlinear model of LRB has been developed that can capture the complex behavior of LRBs at low and high shear strains under seismic loading. The following conclusions are derived from this study:

- The developed analytical model has been validated against experimental results and has demonstrated significantly high accuracy in predicting the behavior of LRBs.
- The hysteresis curves obtained from the experimental model and the proposed model have been compared, and the proposed model has shown remarkable accuracy in predicting the effective stiffness value for the first seven cycles and the effective damping ratio for the first four cycles at the low strain rate and all cycles at large strain rate.
- The accuracy of the proposed model in predicting effective damping ratio and effective stiffness decreases as the number of cycles increases at low strain rate. While the effective stiffness is similar at various cycle and effective damping ratio accuracy is increased after the first cycle at large strain rate.
- The developed analytical model will provide valuable insights into the behavior of LRBs and contribute to the design and analysis of base-isolated structures.

ACKNOWLEDGMENTS

The Natural Sciences and Engineering Research Council (NSERC) of Canada supported this study through the Discovery Grant. The financial support is highly appreciated.

REFERENCES

- [1] Billah, A. H. M. M., and Todorov, B. (2019), “Effects of Subfreezing Temperature on the Seismic Response of Lead Rubber Bearing Isolated Bridge”. *Soil Dynamics and Earthquake Engineering*, 126, 105814.
- [2] Ozdemir, G., Avsar, O., and Bayhan, B. (2011), “Change in Response of Bridges Isolated with LRBs Due to Lead Core Heating”. *Soil Dynamics and Earthquake Engineering*, 31(7), 921–929.
- [3] Rahman Bhuiyan, A., and Alam, M. S. (2013), “Seismic Performance Assessment of Highway Bridges Equipped with Superelastic Shape Memory Alloy-Based Laminated Rubber Isolation Bearing”. *Engineering Structures*, 49, 396–407.
- [4] Turkington, D. H., Cooke, N., Moss, P. J., and Carr, A. J. (1989), “Development of a Design Procedure for Bridges on Lead-Rubber Bearings”. *Engineering Structures*, 11(1), pp. 2–8.
- [5] Kilborn, J., Harn, R., and Firat, Y. (2012), “Seismic Retrofit of Piers Supported on Battered Piles Using Lead-Rubber Bearings”. *12th Triannual International Conference on Ports*. 71–80.
- [6] Bouc, R. (1967), “Forced Vibration of Mechanical Systems with Hysteresis,” *Fourth Conference on Nonlinear Oscillations*, Prague, Czech Republic: Academia.
- [7] Wen, Y.-K. (1976), “Method for Random Vibration of Hysteretic Systems”. *Journal of the Engineering Mechanics Division*, 102(2), pp. 249–263.
- [8] Casciati, F. (1989), “Stochastic Dynamics of Hysteretic Media”. *Structural Safety*, 6(2), pp. 259–269.
- [9] Kikuchi, M., and Aiken, I. D. (1997), “An Analytical Hysteresis Model for Elastomeric Seismic Isolation Bearings”. *Earthquake Engineering & Structural Dynamics*, 26(2), pp. 215–231.
- [10] Kalpakidis, I. V., and Constantinou, M. C. (2009), “Effects of Heating on the Behavior of Lead-Rubber Bearings. II: Verification of Theory”. *Journal of Structural Engineering*, 135(12), 1450–1461.
- [11] Kalpakidis, I. V., and Constantinou, M. C. (2009), “Effects of Heating on the Behavior of Lead-Rubber Bearings. I: Theory”. *Journal of Structural Engineering*, 135(12), 1440–1449.
- [12] Eem, S., and Hahm, D. (2019), “Large Strain Nonlinear Model of Lead Rubber Bearings for beyond Design Basis Earthquakes”. *Nuclear Engineering and Technology*, 51(2), 600–606.
- [13] Marquez, J. F., Mosqueda, G., and Kim, M. K. (2021), “Modeling of Lead Rubber Bearings under Large Cyclic Material Strains”. *Journal of Structural Engineering*, 147(11), 04021170.
- [14] Chen, P., Wang, B., Zhang, Z., Li, T., and Dai, K. (2023), “A Generalized Model of Lead Rubber Bearing Considering Large Strain Stiffening and Degradation”. *Engineering Structures*, 275, 115264.
- [15] Kalpakidis, I. V. (2008), *Effects of Heating and Load History on the Behavior of Lead -Rubber Bearings*. University of New York at Buffalo, US.
- [16] Kumar, M., Whittaker, A. S., and Constantinou, M. C. (2014), “An Advanced Numerical Model of Elastomeric Seismic Isolation Bearings”. *Earthquake Engineering & Structural Dynamics*, 43(13), 1955–1974.
- [17] Park, Y. J., Wen, Y. K., and Ang, A. H.-S. (1986), “Random Vibration of Hysteretic Systems under Bi-Directional Ground Motions”. *Earthquake Engineering & Structural Dynamics*, 14(4), 543–557.
- [18] Grant, D. N., Fenves, G. L., and Whittaker, A. S. (2004), “Bidirectional Modelling of High-Damping Rubber Bearings”. *Journal of Earthquake Engineering*, 8(sup001), 161–185.
- [19] Ozdemir, H. (1976), *Nonlinear Transient Dynamic Analysis of Yielding Structures*. University of California, Berkeley, US.